Preparation and Characterization of Porous-Walled Hollow Glass Microspheres

Fabienne C. Raszewski*, Erich K. Hansen, Ray F. Schumacher and David K. Peeler

Savannah River National Laboratory, Process Science and Engineering Section, Aiken, SC 29808

Porous-walled hollow glass microspheres (PWHGMs) of a modified alkali borosilicate composition have been successfully fabricated by combining the technology of producing hollow glass microspheres (HGMs) with the knowledge associated with porous glasses. HGMs are first formed by a powder glass - flame process, which are then transformed to PWHGMs by heat treatment and subsequent treatment in acid. Pore diameter and pore volume are most influenced by heat treatment temperature. Pore diameter is increased by a factor of 10 when samples are heat treated prior to acid leaching; 100 Å in non-heat treated samples to 1000 Å in samples heat treated at 600°C for 8 hours. As heat treatment time is increased from 8 hours to 24 hours there is a slight shift increase in pore diameter and little or no change in pore volume.

I. Introduction

Hollow glass microspheres (HGMs) are typically produced by a flame forming process, in which a pre-fabricated glass frit containing a blowing agent is passed through a flame at high temperature.[1-3] The decomposition of the blowing agent results in the generation of gases, which cause the glass particles to expand. Spherical glass shells (or HGMs) are formed due to surface tension. The diameter and wall thickness of the HGM is highly dependent on the process conditions, such as flame temperature, residence time in the flame, etc., as well as the composition, viscosity and blowing agent content of the incoming feed.

Production of porous-walled hollow glass microspheres (PWHGMs) combines the existing

* Author to whom correspondence should be addressed. e-mail: fabienne.raszewski@srnl.doe.gov
This work was financially supported by the Savannah River National Laboratory (SRNL) Laboratory Directed Research and Development (LDRD) program.

technology of HGMs with the knowledge associated with spinodal decomposition in phase separated glasses used to develop porous glasses.[4-6] In general, a glass composition prone to amorphous phase separation, such as one within the alkali borosilicate system, is used to produce HGMs. HGMs are then transformed into PWHGMs by a method similar to the Vycor® process.[7-9] A thermal heat treatment is necessary to develop the interconnected microstructure whose scale depends on the duration of the heat treatment. During the acid leaching process, the non-durable, alkali-rich borate phase is removed leaving behind a sponge-like glass shell composed primarily of silica. PWHGMs are characterized by channels and openings that can permit the transport of species of interest into and out of the HGMs as shown in Fig. 1. Heat treatment of the HGMs prior to acid leaching influences the number, shape and size of the pores.[10]

The primary objective of this study is to obtain a fundamental understanding of the compositional and/or heat treatment (time and/or temperature) effects on pore morphology, size and/or pore distribution. The ability to control the microstructure of the PWHGMs provides the opportunity to design a tailored PWHGM system to accommodate different additives or fill agents. Other key physical attributes for PWHGMs that could play a significant role in defining specific applications include strength of the porous shell as well as wall thickness; however, these factors were not evaluated in this study. Applications of these types of systems could range from hydrogen storage, molecular sieves, drug and bioactive delivery systems, to environmental, as well as chemical and biological indicators, relevant to Energy, Environmental Processing and Homeland Security fields.

II. Experimental Procedure

(1) Glass Fabrication

The baseline glass composition of this study is essentially an alkali borosilicate glass in the

Vycor® region that has been slightly modified in order to produce HGMs. This composition was chosen as the baseline for this study as it has been previously shown to successfully produce PWHGMs.[11] Two primary chemical parameters were varied: the silica concentration (±3 wt% and ±6 wt%) and the *molar* B/R ratio (±0.5), which is the ratio of the B_2O_3 content and the alkali oxide content (R_2O, where R=Na and Li).

Glass samples were prepared in approximately 600 g batches using reagent-grade oxides, carbonates and salts. Raw materials were thoroughly mixed and placed into two, 95% Pt / 5% Rh 600 mL crucibles. The crucibles were placed into a furnace at room temperature and linearly ramped to 1300°C. After an isothermal hold at 1300°C for 1 to 3 hours, the crucibles were removed from the furnace and the glasses were poured onto a clean, stainless steel plate and allowed to air cool (quench). The glasses were crushed, blended together, placed into a single 600 mL crucible and re-melted at 1300°C for 1 hour to promote homogeneity in the final glass. Glass from the final melt was poured onto a clean, stainless steel plate and allowed to air cool.

(2) HGM Formation and Separation

Glass from the final melt was ground either with a mechanical grinder or ball mill and sized to 10 – 44 μm. HGMs were formed by a flame forming process using an experimental apparatus designed at the Savannah River National Laboratory (SRNL). Sized particles were passed through a flame (~1200°C) and expanded to spherical, hollow glass shells as gas evolved during the decomposition of the blowing agent.[12,13] HGMs were quenched with water and collected in pails along with any other products resulting from the flame process (i.e. feed particles, solid glass spheres and broken HGMs). To the extent possible, forming conditions, such as powder feed rate, gas/air ratio, and quench water flow rate were kept constant throughout the study. HGMs were separated from other material by a flotation technique.

For each batch of frit, an estimate HGM yield was calculated. HGM yield is defined as a percentage of the total mass of HGMs recovered from the flame process as shown by,

$$HGM\ Yield\ (\%) = \frac{HGMs\ Recovered\ (g)}{HGMs\ Recovered\ (g) + Sinking\ Material\ (g)} \cdot 100$$

where *Sinking Material* refers any of the other products of the flame forming process, such as feed particles, solid glass spheres and broken HGMs. It should be noted that a certain degree of error in this calculation exists as material is lost throughout each step of the process (i.e. flame forming process, separation, filtration, drying, etc.).

(3) PWHGM Preparation

HGMs were treated for 8 hours at 600°C. In addition, baseline HGM samples were also treated for 24 hours at 600°C, and 8 hours and 24 hours at 580°C. Higher heat treatment temperatures (e.g. 620°C) were avoided due to the formation of HGM agglomerates (bonding among the individual HGMs) that could not be separated without creating additional breakage. After each heat treatment, HGMs were allowed to air cool and screened to less than 177 μm.

Heat treated, as well as non-heat treated[†] HGMs were processed in a hot hydrochloric acid solution, followed by a wash with water to remove acid. Any HGMs that remained floating after the acid treatment were collected prior to washing with water, leaving only the PWHGMs (sinking particles) in the vessel; development of pores within the wall due to acid leaching causes the interior void space to become filled with liquid, thus forcing the PWHGM to sink.[‡] PWHGMs were then processed with dilute sodium hydroxide solution in an attempt to remove any gel layer that had formed on the surface during the acid leaching process. The final step consisted of a rinse with de-ionized water.

[†] In order to make microstructural comparisons, as-fabricated (non-heat treated) HGMs were also treated in acid.
[‡] It should be noted that the sinking material would also consist of broken fragments as well as whole PWHGMs. The ratio of broken fragments to whole PWHGMs is unknown at this time.

PWHGM yield was also estimated and is defined as the percentage of PWHGMs recovered from the acid leaching process as shown by,

$$PWHGM\ Yield\ (\%) = \frac{PWHGMs\ Recovered\ (g)}{Initial\ Amount\ of\ HGMs\ (g)} \cdot 100 \quad (2)$$

As in the HGM yield calculation, there is also some uncertainty in this yield equation as there is loss of material during leaching, separations and drying, as well as the presence of fragments in the recovered PWHGMs.

(4) Characterization

Viscosity was measured as a function of temperature using a Brookfield DV-II+ high temperature spindle viscometer of each as-fabricated glass sample.[14]

The true density of the HGMs was measured using gas pycnometry under a nitrogen atmosphere with a Quantachrome Stereopycnometer. The system was calibrated before each set of measurements using a stainless steel sphere of known volume supplied by the manufacturer.

Particle size distribution was determined by separating a known mass of HGMs into various size fractions using an ATM Ultrasonic Sifter and ASTM sieves.

PWHGMs were viewed with a Hitachi HD2000 Scanning Transmission Electron Microscope using a 200 kV acceleration voltage. Samples were prepared in a resin and cut into discs (90 – 100 nm thick) using a Reichert – Jung UltraCut E Microtome.

Pore volume, size and distribution were determined via mercury porosimetry using a Micromeritics AutoPore IV 9500 (V1.07).

III. Results and Discussion

(1) HGM Yield

HGM yields as a function of SiO_2 and B_2O_3 content are shown in Figs. 2 and 3. Viscosity data at 1200°C as a function of glass composition are shown for reference; this temperature was

chosen as it is the approximate temperature of the flame during the HGM forming process. The baseline composition has the highest yield; however, it appears that the maximum yield may occur between 60 and 63 wt% SiO_2 with a molar B/R ratio in the range of 0 and -0.5. A considerable decrease in yield is observed as the SiO_2 content is raised from 63 to 66 wt% and when the molar B/R ratio is increased by 0.5 relative to the baseline composition. There is a continuous increase in viscosity as the SiO_2 content is raised from 54 wt% to 66 wt% and a slight increase as the B/R ratio is raised from -0.5 to +0.5. One would expect that yield decreases with increasing viscosity since lower viscosities are typically more desirable for spheroidization. The data suggest that the relationship between yield, viscosity and composition may be more complex; yield data is parabolic with composition whereas viscosity data is linear. While it appears that phase separation does not influence the viscosity of these glasses, it is possible that phase separation does impact the ease of HGM formation depending on the location with the immiscibility dome.

(2) Particle Size Distribution

In general, a high percentage of HGMs have diameters within the range of 45 – 75 μm, which is to be expected as the feed material is sized to 10 – 44 μm. Unlike any of the other compositions, the HGMs with a SiO_2 content of 66 wt% (+6 SiO_2) have a high fraction of small HGMs, with diameters less than 45 μm. HGMs with a varied B/R molar ratio of ±0.5 were not measured. It is possible that the relatively high silica content and higher viscosity of this glass does not promote blowing during HGM formation, thus producing HGMs of smaller diameters.

(3) Density

The true densities of the HGMs are shown as a function of SiO_2 and B_2O_3 content in Fig. 4. In general, the densities increase linearly with SiO_2 content. For the same SiO_2 content, the densities of the B/R ±0.5 compositions increase with B_2O_3 content. In both curves, the density of the baseline

composition is a little low compared to the linear fit of the data. This anomaly may be due to: i) instrumental error and/or ii) effectiveness of blowing during the flame process with this particular composition; however, neither of these explanations seem plausible at the present time. As all of these glasses are primarily composed of glass formers (SiO_2 and B_2O_3), it is expected that density is influenced by the changes in the glass former content. Minor variations in alkali and alkaline earth content should not have a significant or measurable effect. Density is also not influenced by phase separation as density is a result of the averaged volumes of the phases present.

(4) PWHGM Yield

PWHGM yield[§] as a function of silica content for non-heat treated samples and samples treated at 600°C for 8 hours are shown in Fig. 5. There does not appear to be a trend in the yield as a function of composition for either set of data. PWHGM yield remains relatively constant with changes in SiO_2 content in either the non-heat treated and treated at 600°C for 8 hours samples. The -3 SiO_2 (non-heat treated) and +3 SiO_2 (heat treated at 600°C for 8 hours) samples have yields are abnormally high; however, these samples retained a lot of moisture, even after drying at 90°C overnight, and thus only appear to have superior yields. Additional drying was not performed to provide more realistic yield data for these two systems. It is expected that if properly dried, the yields would be within the range of the other samples. There is an observable increase in yield when the HGMs are heat treated prior to acid leaching (i.e., a comparison of non-heated to heat treated yields for a fixed composition). Although not shown, there does not appear to be any difference in yield of the baseline PWHGMs as the heat treatment time is increased from 8 hours to 24 hours or when the heat treatment temperature is raised from 580°C to 600°C. In general, implementation of

[§] As mentioned in Section II, there are a number of processing steps that can contributed to errors that influence the accuracy of the yield calculation as PWHGMs are produced from HGMs. Thus, the yields discussed in this section are only approximate values. Actual values may be lower or higher depending on the quantity of PWHGMs lost during acid leaching and the quantity of moisture in the PWHGMs after drying.

an 8 or 24 hour heat treatment (compared to no heat treatment) results in a coarsening of the microstructure, i.e. more of the highly soluble, silica-poor phase is available for removal. Thus, a higher fraction of material is leached during the acid treatment and more PWHGMs are formed (yield increases).

(5) Microstructure of PWHGMs

Please note that only the microstructures of the baseline composition will be discussed.

A comparison of the microstructures of a non-heat treated and heat treated PWHGM prior to acid leaching is shown in Fig. 6. While the non-heat treated sample is porous (Fig. 6a), the pores are barely observable at high magnification. There is a considerable difference in the porosity of the sample heat treated at 600°C for 8 hours (Fig. 6b); the interconnected microstructure is clearly defined and the porosity can easily be observed at lower magnification. As the heat treatment time is increased from 8 hours to 24 hours (at a fixed heat treatment temperature of 580°C), there is very little change in the microstructure of the baseline composition as shown in Figs. 6c and 6d. It is possible that a heat treatment time less than 8 hours would yield a microstructure similar to that found in the samples treated for 8 hours; however, treatment times other than 8 hours and 24 hours were not investigated at this time. The microstructural trends observed at 580°C as a function of heat treatment time are comparable at a heat treatment temperature of 600°C. Coarsening of the microstructure occurs as the heat treatment temperature is raised from 580°C to 600°C as shown in Figs. 6b and 6c. Significant differences in the resulting microstructure are evident with only a 20°C change in heat treatment temperature.

(6) Porosity

Mercury porosimetry curves for various samples of the baseline composition are shown in Fig. 7. The y-axis, log differential intrusion volume is calculated by dividing the difference in

volume (V) by the difference in the logarithms of diameters (D) and is given by[15]:

$$\frac{\Delta V}{\Delta \log D} = \frac{V_{i+1} - V_i}{\log D_{i+1} - \log D_i} \tag{3}$$

The x-axis is simply the log of the pore diameter. Peak area is a representation of pore volume.

While the non-heat treated sample consists of a high fraction of pores that are approximately 100 Å in diameter (refer to Fig. 6a), heat treatment at 600°C (both 8 hours and 24 hours) causes the pore diameter to increase to approximately 1000 Å (refer to Fig. 6b), confirming the microscopy results. There is little variation in the porosity as the heat treatment time is increased from 8 hours to 24 hours for the sample treated at 600°C; a very slight shift in pore diameter is observed and very little increase (if any) in pore volume, also confirming the microscopy results. Mercury porosimetry results are inconclusive for the samples treated at 580°C.

These results, along with the microscopy images, suggest that heat treatment *times* used in this task are not as effective as the heat treatment *temperatures* in changing the porosity (or phase separation) in HGMs and the resulting PWHGMs.

IV. Conclusions

HGMs of a modified alkali borosilicate composition were fabricated by a flame forming process using an experimental apparatus designed and constructed at SRNL. Average diameters are in the range 45 – 75 μm and yield is maximized in the baseline composition (85%). Density of the HGMs is 0.369 – 0.744 g/cc and increases linearly with increasing SiO_2 and B_2O_3 content. PWHGMs were formed by a method similar to the Vycor® process. Yield is unaffected by the SiO_2 content, but increases, in general, when the HGMs are heat treated prior to acid leaching. Porosity has been found to be most influenced by heat treatment temperature as opposed to the duration of the heat treatment. Pore diameter is increased by a factor of 10, from 100 Å in non-heat treated samples to 1000 Å in samples heat treated at 600°C for 8 hours. As the heat treatment time is increased from

8 hour to 24 hours, there is only a slight shift in pore diameter and little or no increase in pore volume.

Acknowledgements

The authors would like to thank Scott W. Gaylord, Nathan A. Carlie, Laeticia Petit and Kathleen A. Richardson at the Advanced Materials Research Laboratory at Clemson University for capturing the scanning electron microscope images, as well as Micromeritics Analytical Services for measuring the porosity of our samples.

References

[1]W. R. Beck and D. L. O'Brien, "Glass Bubbles Prepared by Reheating Solid Glass Particles," U.S. Pat. 3,365,315,
[2]P. Garnier, D. Abriou, and M. Coquillion, "Process for Producing Glass Microspheres," U.S. Pat. 4,661,137,
[3]P. A. Howell, "Glass Bubbles of Increased Collapse Strength," U.S. Pat. 4,391,646,
[4]P. R. Anderson, "Hollow Microspheres with Wall through-Openings," European Patent EP0150288, 1985.
[5]R. F. Schumacher, G. G. Wicks, and L. K. Heung, "Hollow Porous Glass Microspheres for Hydrogen Storage," U.S. Pat. Application 20060060820,
[6]W. Vogel, "Chemistry of Glass," pp. 69-95. Columbus, OH: The American Ceramic Society. (1985).
[7]H. P. Hood and M. E. Nordberg, "Treated Borosilicate Glass," 2,106,744,
[8]H. P. Hood and M. E. Nordberg, "Method of Treating Borosilicate Glasses," United States 2,215,039,
[9]H. P. Hood and M. E. Nordberg, "Borosilicate Glass," 2,221,709,
[10]F. Janowski and D. Enke, "Porous Glasses," pp. 1432-1542. In *Handbook of Porous Solids,* **Vol. 3.** Edited by F. Schuth, K. S. Sing, and J. Weitkamp. Wiley-VCH, Weinheim, Germany, 2002.
[11]R. F. Schumacher, G. G. Wicks, and L. K. Heung: Unpublished work. (2005).
[12]C. D. Hendricks, "Glass Spheres," pp. 149168. In *Glass: Science and Technology*, **Vol. 2.** Edited by D. R. Uhlmann and N. J. Kreidl. Academic Press, New York, NY, 1984.
[13]C. D. Hendricks, "Glass Spheres," pp. 418-422. In *Ceramics and Glass,* **Vol. 4.** Edited by S. J. Schneider, Jr. ASM International, Materials Park, OH, 1991.
[14]"Standard Practice for Measuring Viscosity of Glass above the Softening Point." In**.** ASTM International, West Conshohocken, PA, 2007.
[15]P. A. Webb and C. Orr, "Pore Structure by Mercury Intrusion Porosimetry," pp. 181-186. In *Analytical Methods in Fine Particle Technology***.** Micromeritics Instrument Corporation, Norcross, GA, 1997.

Figure 1. Conceptual representation of a PWHGM.

Figure 2. HGM yield and viscosity (at 1200°C) as a function of SiO2 content. Lines are a guide to the eye.

Figure 3. HGM yield and viscosity (at 1200°C) as function of B2O3 content. Lines are a guide to the eye.

Figure 4. HGM density as a function of SiO_2 and B_2O_3 content. Lines are a guide to the eye.

Figure 5. PWHGM yield as a function of SiO2 content. Lines are a guide to the eye.

Figure 6. Microstructures of baseline PWHGMs with the following heat treatments prior to acid leaching, (a) non – heat treated, (b) 600°C for 8 hours, (c) 580°C for 8 hours and (d) 580°C for 24 hours.

Figure 7. Porosity as a function of heat treatment conditions for the baseline composition.

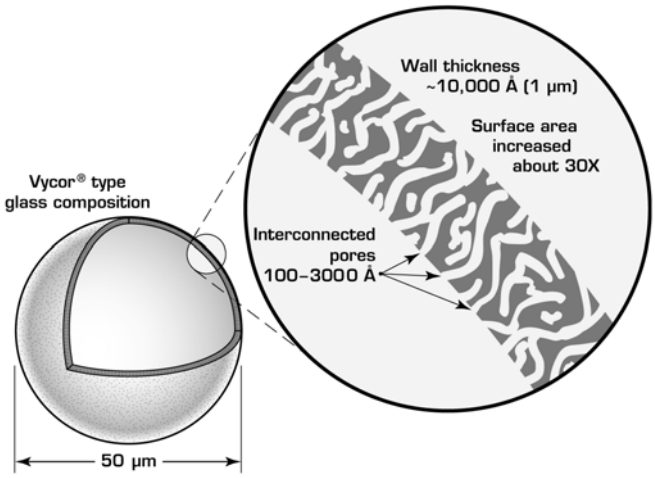

Figure 1. Conceptual representation of a PWHGM.

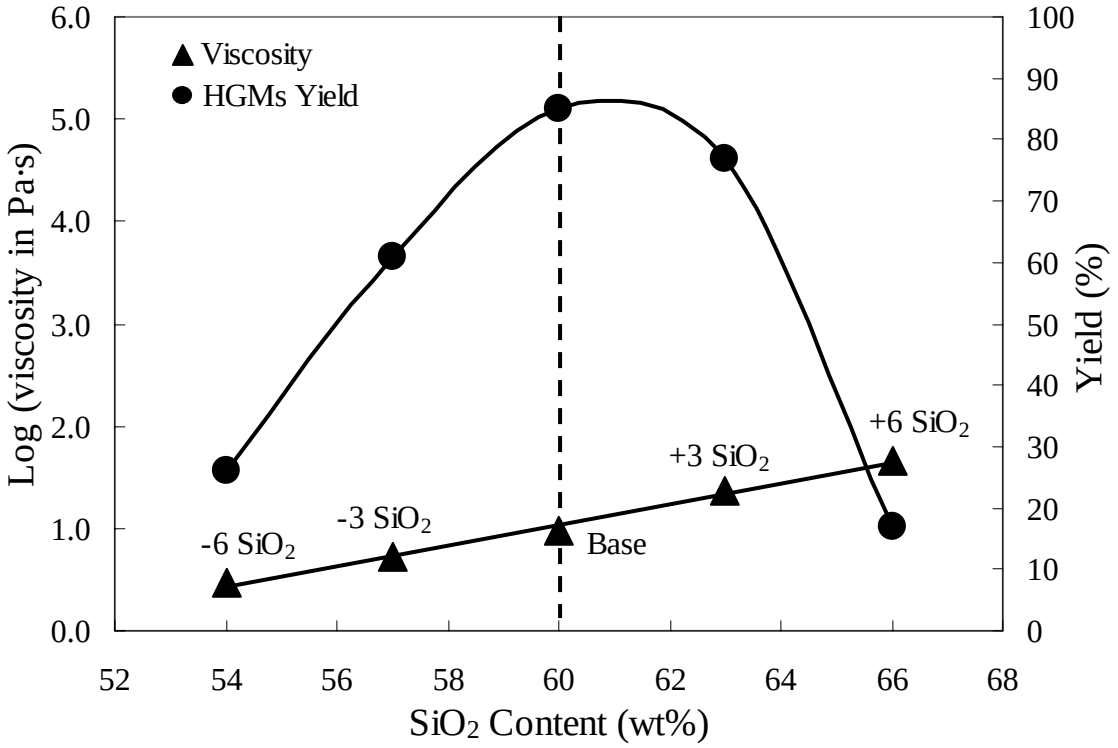

Figure 2. HGM yield and viscosity (at 1200°C) as a function of SiO_2 content. Lines are a guide to the eye.

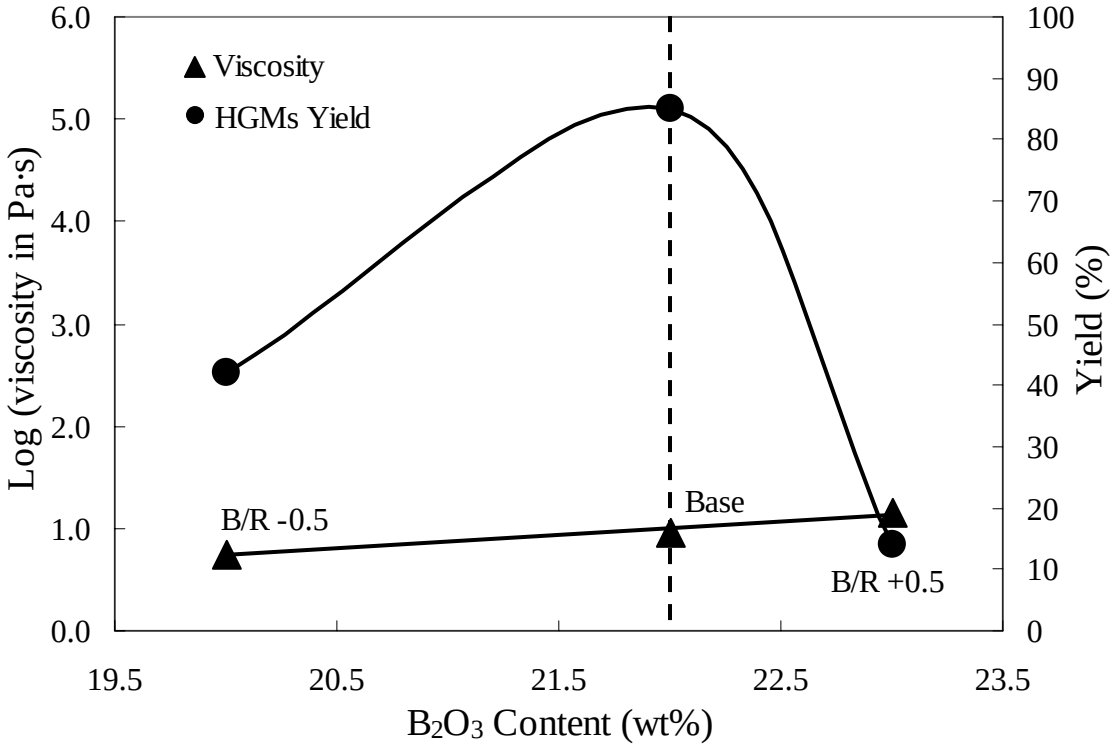

Figure 3. HGM yield and viscosity (at 1200°C) as function of B_2O_3 content. Lines are a guide to the eye.

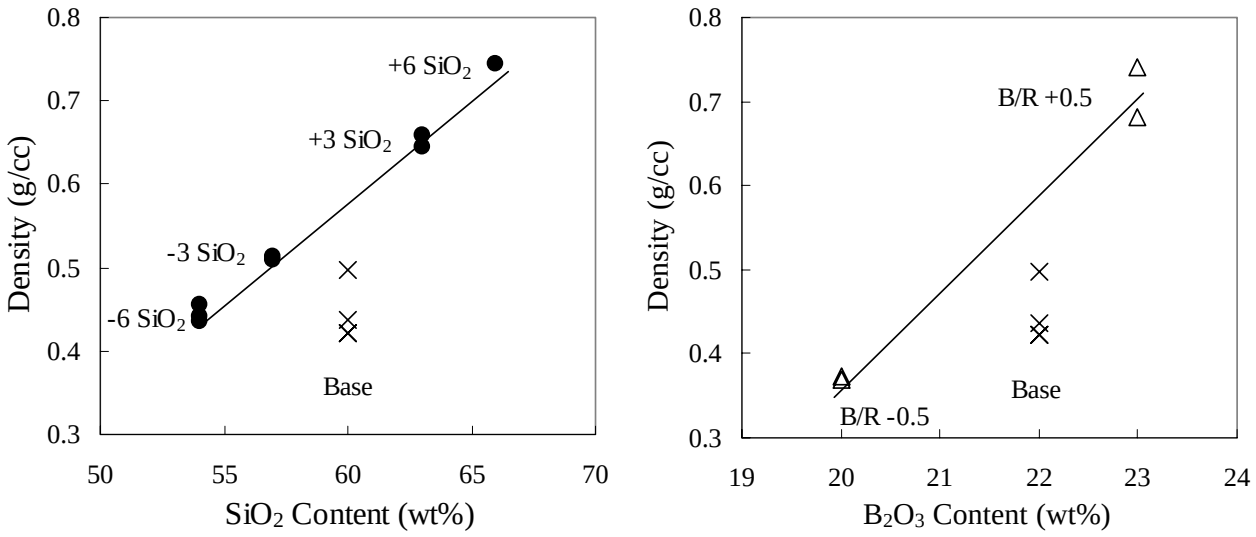

Figure 4. HGM density as a function of SiO_2 and B_2O_3 content. Lines are a guide to the eye.

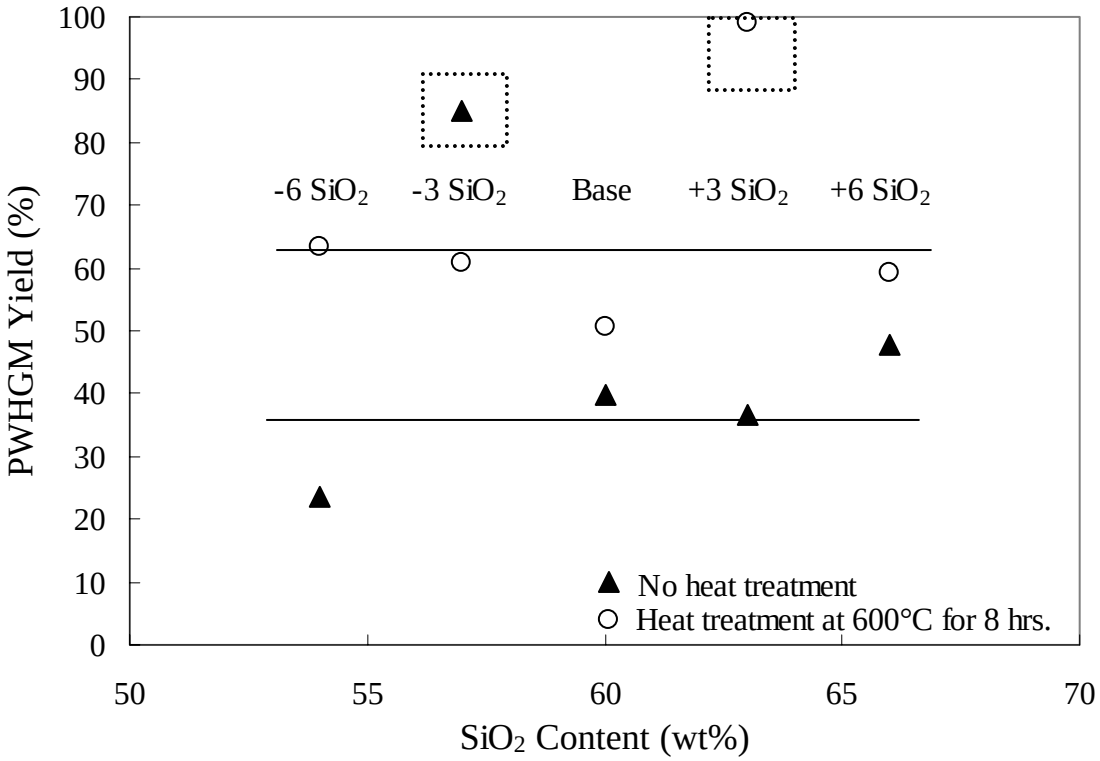

Figure 5. PWHGM yield as a function of SiO_2 content. Lines are a guide to the eye.

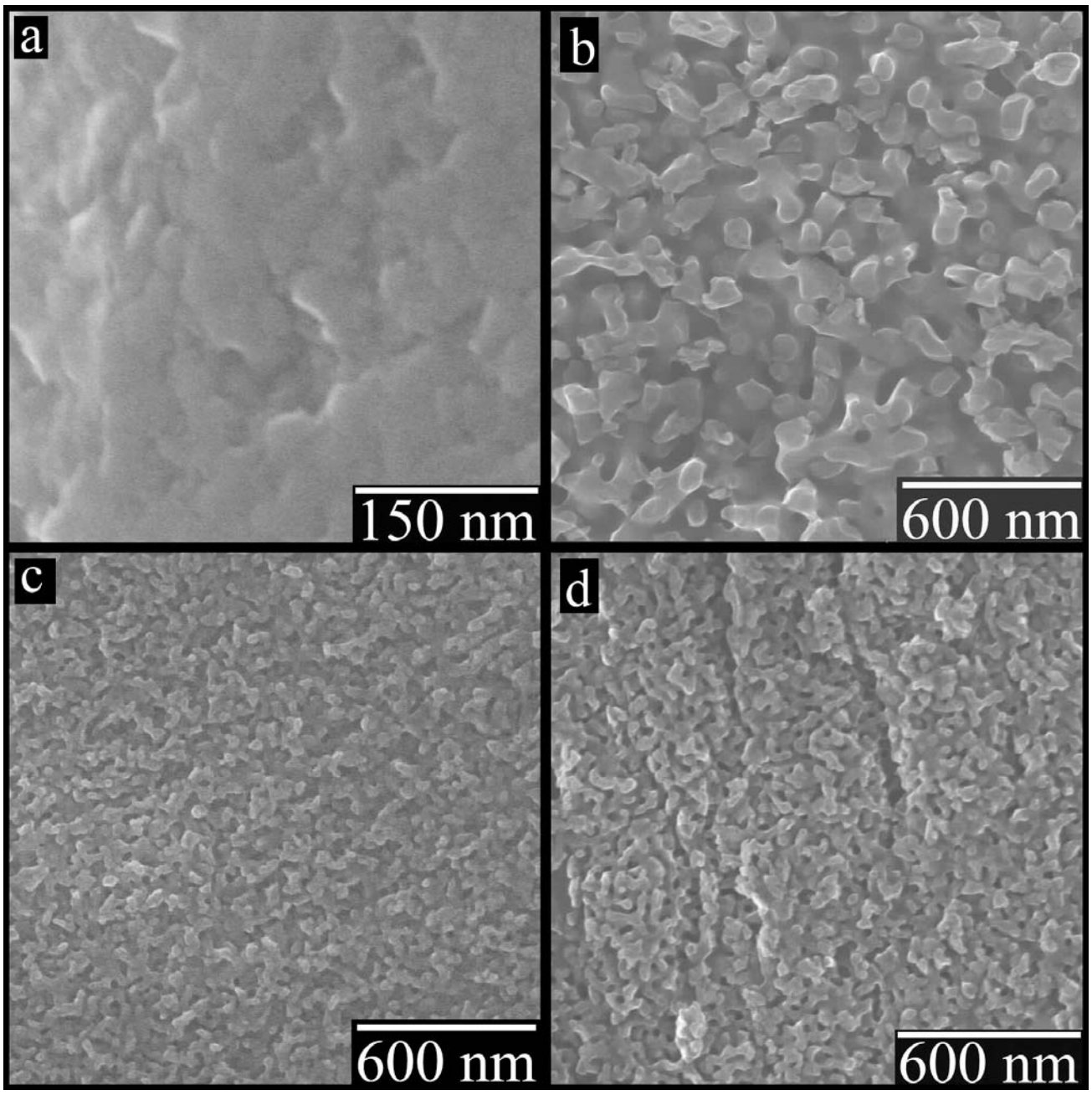

Figure 6. Microstructures of baseline PWHGMs with the following heat treatments prior to acid leaching, (a) non – heat treated, (b) 600°C for 8 hours, (c) 580°C for 8 hours and (d) 580°C for 24 hours.

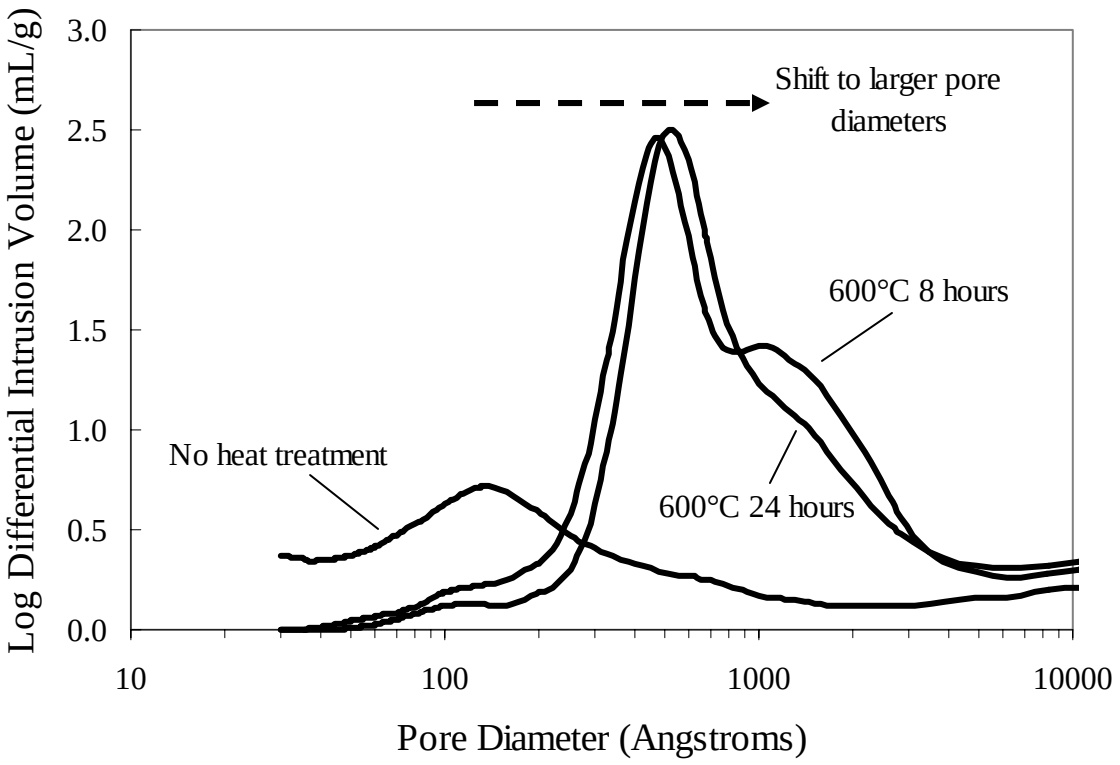

Figure 7. Porosity as a function of heat treatment conditions for the baseline composition.